Engineering models for merging wakes in wind farm optimization applications

2015 J. Phys.: Conf. Ser. 625 012037

(http://iopscience.iop.org/1742-6596/625/1/012037)

Journal of Physics: Conference Series **625** (2015) 012037 doi:10.1088/1742-6596/625/1/012037

Engineering models for merging wakes in wind farm optimization applications

E. Machefaux[1], G.C. Larsen[1] and J.P. Murcia Leon [1]

[1] DTU Wind Energy, Frederiksborgvej 399, 4000 Roskilde, Denmark

E-mail: ewma@dtu.dk

Abstract. The present paper deals with validation of 4 different engineering wake superposition approaches against detailed CFD simulations and covering different turbine interspacing, ambient turbulence intensities and mean wind speeds. The first engineering model is a simple linear superposition of wake deficits as applied in e.g. Fuga. The second approach is the square root of sums of squares approach, which is applied in the widely used PARK program. The third approach, which is presently used with the Dynamic Wake Meandering (DWM) model, assumes that the wake affected downstream flow field to be determined by a superposition of the ambient flow field and the dominating wake among contributions from all upstream turbines at any spatial position and at any time. The last approach developed by G.C. Larsen is a newly developed model based on a parabolic type of approach, which combines wake deficits successively. The study indicates that wake interaction depends strongly on the relative wake deficit magnitude, i.e. the deficit magnitude normalized with respect to the ambient mean wind speed, and that the dominant wake assumption within the DWM framework is the most accurate.

1. Introduction

Wind farm flow fields remain a challenging topic, which has attracted increasing attention during the last decade. Considerable progress in the fundamental understanding of such fields has been achieved through analysis of dedicated full-scale and wind tunnel experiments as well as through detailed CFD computations, which in turn has paved the way for development and validation of powerful engineering type of models preserving the essential physics of the problem while at the same time offering a substantial reduction in computational requirements. Computational demands is a critical parameter when it comes to design and optimization of wind farm layout in practice due to the huge number of wind farm flow conditions to be considered.

To remain of practical relevance, the commonly used approach in wind farm design codes is to combine single wake calculations with a recipe for wake superposition to determine the combined characteristics of the merged wake. The main challenge with predicting merged wakes is that, according to Crespo et al. [1], the ambient flow in which a downstream wake diffuses is fundamentally different than the one at upstream locations. Instead, today's commonly used wake superposition techniques rely on simple mathematical rules that are not justified by any physical means.

The present paper aims at evaluating the performance of 4 different wake superposition techniques. The benchmark is performed against results from detailed CFD simulations based on Large Eddy Simulation using the Actuator Disc rotor modeling technique under fully turbulent atmospheric flow. This model has been validated against merged wake lidar measurements as part of the study by Machefaux et al. in [14]. In the present research, merging wakes are

studied with the most simple configuration, where two stall regulated rotors are aligned with the incoming wind, under different turbine spacings, ambient turbulence intensities and mean wind speeds.

One of the most simplistic wake overlapping approaches presently tested is a *linear superposition* of wake deficits, which was first introduced by Lissaman in [12]. As was argued by Crespo et al. [1], that this assumption fails for large perturbations where many upstream wakes are superimposed, as negative velocities may arise.

Thus, Katic et al. in [6] proposed to apply a linear superposition of the squares of the velocity deficits (*quadratic summation* rule). Various investigations showed that this method is beneficial in the case where many wakes are combined, giving better agreement with experimental results than the linear superposition for a small wind farm.

A power production benchmark proposed by Gaumond in [3] and based on the long term experimental observation at the Horns Rev offshore wind farm assessed the performance of these two simplistic approaches. It was found that the quadratic rule of Katic et al. in [6] associated to the standard industry N.O. Jensen wake model [5] may not be suitable for large wind farms, as it fails to capture properly the physic of merging wakes from neighboring rows of turbines.

This conclusion may initially appear contradictory with the observation by Katic [6], however it is not. The quadratic formulation of Katic at al. was tested for experimental data on a small wind farm, while the effect of neighboring wakes merging occurring at a certain downstream distance is only visible in large offshore wind farm as Horns Rev. In the latter observation, the quadratic rule failed to model deep array effects, as it reaches an equilibrium state (where the velocity deficit becomes constant) too quickly.

Recently, as part of the development of the wind farm topology optimization platform TOPFARM [7], two new wake superposition approaches were formulated. The first one is part of the in-house Aeroelastic code HAWC2 ([25]) coupled to the DWM model [8], where overlapping wakes are modeled using the so-called *dominant wake* approach. In this approach, the merged wake at a given location and at a given time in a wind farm is assumed to be characterized by the most dominant deficit of all upstream wakes contribution. In this way, the most attenuated and expanded upstream wakes contributes to the merged wake deficit more than what the conventional quadratic and linear summations would predict. This method proved robust to determine load and power production of the Egmond Aan Zee wind farm, as seen in the study by Larsen at al. in [11], and more recently, for the offshore Lillgrund wind farm [10]. The second technique, presently referred to as the *G.C. Larsen superposition model* [9], is based on a parabolic type of model, which combines wake deficits successively.

Among other observations, the present benchmark revealed that the performance of simple linear and quadratic summation approaches are highly dependent on the thrust force acting on the turbine.

2. Engineering models for predicting merging wakes

2.1. Introduction

In the present paper, we focus on the simplest merging wake configuration, where two turbines are aligned with the mean inflow direction. Specifically, this study aims at evaluating the performance of commonly used engineering models for single wake superposition, in order to predict both the mean deficit and the available aerodynamic power over the rotor area of a "fictitious" third turbine located downstream of the two wake generating rotors. The engineering models benchmark is based on CFD-LES simulations under sheared turbulent atmospheric inflow and covering a range of ambient configurations and turbine spacings, as described subsequently in Section 3.

A sketch of the investigated merging wake configuration is depicted in Fig. 1. The resulting wake deficits at the downstream location of a fictitious turbine $T3$ is obtained from superposition

of single wake deficit generated by turbines $T1$ and $T2$, respectively. The inflow condition to the downwind turbine $T2$ varies with the chosen modeling approach, as will be detailed in Section 2.2.

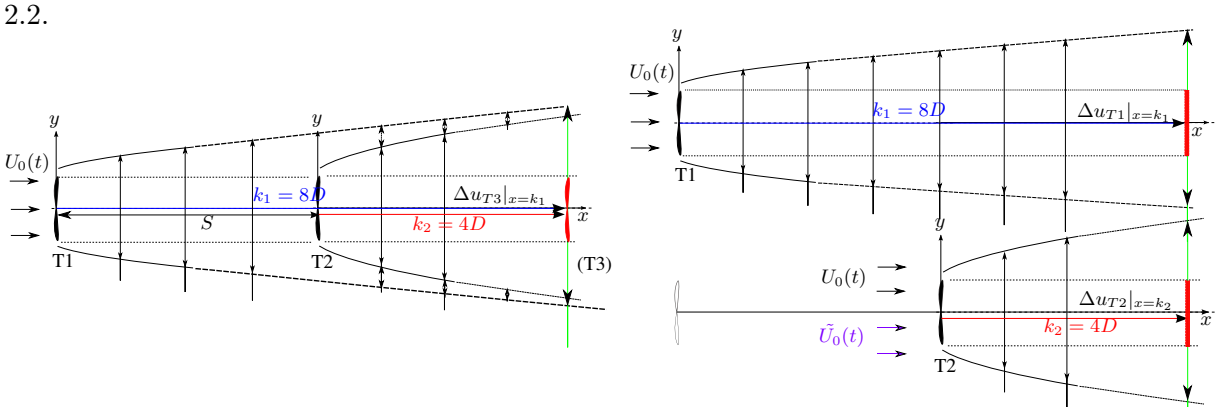

Figure 1. Sketch of the investigated wake overlapping situation. S denotes the turbine inter-spacing. The merged wake deficit (left figure) is decomposed into two single wake contributions: the wake of $T1$ at $k_1 = 8D$ downstream (top right figure); and the wake of $T2$ at $k_2 = 4D$ downstream (bottom right figure), where the origin of the x-axis is located at the most upstream rotor center. U_0 refers to the free stream velocity. Two different assumptions of the inflow conditions of turbine $T2$ are indicated: 1) using the mean wind speed U_0 or 2), using a reduced wind speed $\tilde{U_0}$ characterizing the disturbed incoming wind generated by the wake of $T1$.

We presently defined the wake velocity deficit in its normalized form, (Δu), as:

$$\Delta u = 1 - \frac{u_w}{U_0} \tag{1}$$

where u_w is the velocity in the wake and U_0 is the mean free stream velocity. The corresponding average deficit $\overline{\Delta u}$ over the rotor plane of area A is, in polar formulation, defined as:

$$\overline{\Delta u} = \frac{1}{A}\int_{-\pi}^{\pi}\int_{0}^{R} \Delta u r dr d\theta \tag{2}$$

The numerical evaluation of the integral in Eq. 2 is typically based on either: 1) a trapezoidal integration algorithm or 2); the Gauss integration technique as described in [9], where the averaged deficit is approximated using a forth order Gauss integration.
The corresponding available aerodynamic power P over the rotor plane is then obtained as:

$$P = \frac{1}{2}\rho A\left(U_0\left(1 - \frac{1}{A}\int_{-\pi}^{\pi}\int_{0}^{R}\Delta u r dr d\theta\right)\right)^3 = \frac{1}{2}\rho A\left((1-\overline{\Delta u})U_0\right)^3 \tag{3}$$

where U_0 is the mean free stream velocity. The determination of $\overline{\Delta u}$ varies with the tested engineering models as introduced subsequently.

2.2. The tested engineering models

2.2.1. Simple linear superposition

In this approach, the merged wake deficit at the downstream location corresponding to the $n^{th}+1$ fictitous rotor is obtained from linear superposition of the n upstream single wake deficits evaluated at the downstream location $x(n+1)$. Two assumptions on the characteristic of the inflow condition for the single wake calculations are investigated. The first modeling approach, as used by Lissaman et al. in [12], assumes that the ambient condition is the same for each wake generating turbine and equal to the free stream condition (U_0). The second approach, similar to the one resulting in the linearized CFD model FUGA [20], assumes that the ambient condition of each turbine is based on a reduced wind speed defined by the upstream wake affected inflow

($\tilde{U_0}(n)$). In the latter, the wake generated turbulence is neglected, and thus the turbulence intensity is constant and equal to the free stream one.

The average merged wake deficit resulting from the linear summation of n upstream velocity deficit contributions is then expressed as:

$$\overline{\Delta u}_{n+1} = \sum_{j=1}^{n} \left(\overline{\Delta u}_j|_{x(n+1)} \right) \tag{4}$$

Where in Eq. 4, each single wake contribution Δu_j is evaluated at the downstream location $x(n+1)$. The overbar denotes the averaging operator.

2.2.2. The "quadratic" approach
The quadratic superposition, as applied in the widely used PARK program [6], is obtained as the square root of the sums of the upstream single wakes deficits. Thus, the quadratic summation of n upstream velocity deficit contributions reads:

$$\overline{\Delta u}_{n+1} = \sqrt{\sum_{j=1}^{n} \left(\overline{\Delta u}_j|_{x(n+1)} \right)^2} \tag{5}$$

2.2.3. Multiple wakes in the Dynamic Wake Meandering approach
The superposition of wakes within the DWM model [8], [16] and [11], assumes that the wake affected downstream flow field is determined by a superposition of the ambient flow field and the *dominating* wake among contributions from all upstream turbines at any spatial position and at any time. This approach was motivated by an analysis of the wake deficit from 5 upstream turbines separated by 8 rotor diameters and calculated from the axis symmetric eddy viscosity model described in [16]. This model further assumes that the contributing upstream wakes are independent of each other, and thus, are determined under the same inflow characteristics (mean wind speed and turbulence field).
The superposed deficit in the DWM model is then calculated as:

$$\overline{\Delta u}_{n+1}(t) = MAX(\overline{\Delta u}_i(t))|_{x(n+1)} \tag{6}$$

where i is the upstream turbine index ranging from 1 to n in the park, and t denotes the time instant.

2.2.4. The G.C. Larsen wake superposition model
Finally, the G.C Larsen superposition model (GCL) described in [9] is evaluated in this study. We presently focus only on the wake-rotor interaction as fomulated in [9]. In this model, the instantaneous flow field at a given downstream turbine location x is obtained from the linear summation of all instantaneous single wake contributions at the same location x. Each of these single wake contributions are obtained from independent calculations conducted with an unsteady inflow field including the accumulated upstream wakes. As a result, this unsteady model, similarly to the DWM framework, takes into account the large scale wake meandering displacements.

The instantaneous wake velocity field $U(t)$ at the $n^{th}+1$ rotor in the turbine row is, in the *GCL* model, defined as:

$$U_{n+1}(t) = \overline{U_0} + \sum_{j=1}^{n} (U_j(t)|_{x(n+1)}^{\tilde{U}_j(t)} - \tilde{U}_j(t)) \tag{7}$$

In Eq. 7, each single wake contributions $U_j(t)$ to be superposed are determined at same downstream position $x(n+1)$ as where the resulting merged wake flow field is estimated, and

simulated with the inflow field $\tilde{U}_j(t)$ described subsequently. The corresponding average deficit over the rotor area $\overline{\Delta u}_{n+1}(t)$ is calculated using Eq. 1 and Eq. 2.

The time dependent inflow condition $\tilde{U}_j(t)$ required for the simulations of the j^{th} upstream single wake contribution is defined as:

$$\tilde{U}_j(t) = \overline{U_0} + \sum_{i=1}^{j-1} (U_i(t)|_{x(j)} - \overline{U_0}) \tag{8}$$

where $x(n)$ is the downstream distance from the most upstream rotor.

3. The merging wakes validation data

The present section aims at detailing the model and computational set up used to generate the merging wakes validation data.

3.1. Numerical model and computational set up

The wake velocity field was simulated using detailed unsteady CFD computations. The simulations were conducted using the incompressible Navier-Stokes solver EllipSys3D [18, 19, 23] and combines LES of the flow field with actuator disc modelling of the rotors. The atmospheric turbulence is modelled using the method presented by Troldborg et al. [27], where pre-generated Mann turbulence [17] is inserted in a cross-section upstream of the rotors. The used actuator disc model is based on the actuator shape model [21] combined with a blade element approach, where the aerodynamic loading is determined from the local flow conditions at the disc and 3D corrected aerofoil data as described by Réthoré et al. [22]. The LES model uses a sub grid scale model developed by Ta Phuoc [24], and the used solver parameters are identical to previous work [26, 15, 13].

The simulations are carried out in a regular Cartesian mesh of dimensions ($L_x = 24D_N$, $L_y = 14D_N$, $L_z = 14D_N$), where x, y and z denotes the streamwise, lateral and vertical coordinates, respectively, and D_N denotes the inserted turbine rotor diameter.

The simulated turbine is a stall regulated Nordtank 500 kW turbine, with a rotor diameter of 41 m and a hub height of 36 m. This turbine was chosen for practical reasons, as the rotational speed and the pitch is constant and therefore does not require any additional control. Furthermore, the present numerical model was validated for merging wake situations against full-scale lidar measurements conducted on the Nordtank turbine in [14].

The grid layout and the boundary conditions are in accordance with previous studies [26, 15]. The boundary conditions are as follows: Dirichlet conditions at the inlet and upper boundary ($x = 0$ and $z = 14D_N$), Neumann conditions at the outlet ($x = 24D_N$), symmetry condition at the bottom ($z = 0$), and cyclic boundary conditions on the sides ($y = 0$ and $y = 14D_N$).

In the region around and downstream of the rotors the grid spacing is equivalent to $dx = 60/D_N$ in the lateral and vertical direction, and $dz = 62/D_N$ in the stream-wise direction. The cells are stretched away from the wake region towards the domain boundaries, resulting in a total number of cells of 39.81 millions inside the domain. Each actuator disc is represented with a separate 2D polar grid with 94 radial and 180 angular elements.

The unsteady simulations are conducted using the time step $dt = 0.05s$. Fig. 2 shows an example of the coarse representation of the computational domain seen from the top, and the location of extraction planes.

3.2. Merging wakes parametric study

The present merged wake study involves a simple layout consisting of two Nordtank 500 kW stall regulated turbines (denoted $T1$ and $T2$) associated with a wide variety of ambient conditions. Specifically, two turbine inter-spacings are tested: a 'small' spacing of 4 rotor diameters,

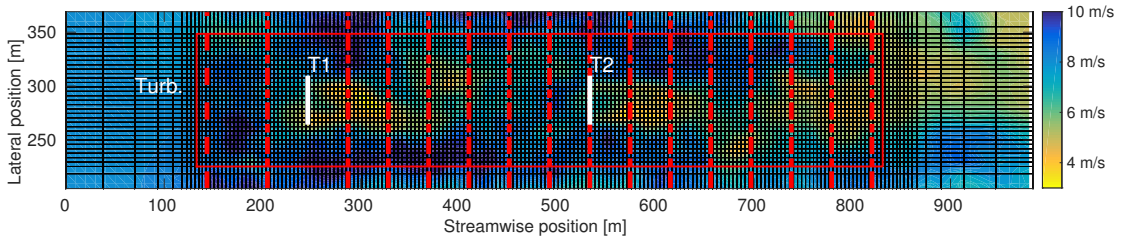

Figure 2. Coarse representation of the computational domain seen from the top. The white lines correspond to the wake of turbine $T1$ and $T2$ separated from 7 rotor diameters. Dash red lines are wake cross sections extracted at 5Hz and at a resolution of 1 m. The red rectangle shows a longitudinal extraction plane at hub height. The instantaneous streamwise velocity field is shown in the background where blue colors indicate regions of high wind speed and yellow colors show the wake region.

corresponding to a rather severe wake condition similar to the Middelgrunden wind farm outside Copenhagen harbor; and a 'larger' 7 diameters spacing, which is typical for offshore wind farm layouts in general. Additionally, two simulated ambient turbulence intensities are adopted, corresponding to typical offshore and onshore values of respectively 6% and 12%. Finally, four mean wind speeds are chosen covering different turbine loadings and thus various wake flow regimes. Table 1 summarizes the test matrix. The inflow wind profile is assumed neutral and modeled using a logarithmic law, where the roughness is equal to 5 cm. The friction velocity is adjusted to satisfy the prescribed hub height wind speed for all cases. Finally, synthetic Mann turbulence are generated using the same seed but scaled to match the required turbulence intensity and sheared inflow profile.

Table 1. Merging wake parametric study. Test cases matrix. The turbulence intensity corresponds to the free stream turbulence intensity I_{ref}, as resolved by the CFD-LES computations.

	5 m/s		**8 m/s**		**11 m/s**		**15 m/s**	
Merged wake: 4D spacing	6.3%	12.2%	6.3%	11.9%	6.3%	11.9%	6.4%	12.1%
Merged wake: 7D spacing	6.3%	12.2%	6.3%	11.9%	6.3%	11.9%	6.4%	12.1%

3.3. Simulation of the single wake contributions

The benchmark of merging wake models further requires, in addition to the simulations performed with both rotors, to determine the two turbine single wakes, independently. However, the tested wake accumulation models are based on various inflow field assumptions formulated in either instantaneous or average terms. This section therefore aims at describing the way each engineering model are related to the available LES computations.

3.3.1. Single wake definition in the DWM wake superposition framework

As described in [11], the DWM model assumes that the superposed single wake contributions are not influenced by other upstream wakes, and thus, can be simulated at the same unsteady inflow conditions. However, the DWM wake accumulation model is formulated in instantaneous terms (Eq. 6) so that the merged wake deficit at any downstream location is obtained from the instantaneous dominant wake among all upstream contributions. Therefore, it is crucial to ensure that the single wake contributions are simulated within the same large scale in the turbulence flow field, to ensure spatial and temporal correlation between the merged and the two independent single wake simulations.

The assumption of constant inflow for each of the turbines in the propagation row simplify the analogy with LES simulation. Specifically, only one single wake computations is required for the application of the DWM superposition, as the multiple turbine wakes can be analyzed

by simply extracting the instantaneous velocity field at different downstream cross section, i.e.:

$$\Delta u_n(t)|_{x(n+1)}^{U_0(t)} \equiv \Delta u_{n+1}(t+dt)|_{x(n+2)}^{U_0(t)} \tag{9}$$

However, this analogy can be only applied after introducing a relevant time shit dt for each instantaneous deficit characterizing their respective distance from the wake emitting rotor, or more specifically from the upstream location where the Mann turbulence are inserted into the computational domain. The Taylor frozen turbulence hypothesis is adopted to quantify this time shift as $dt = S/\overline{U_0}$, where S is the turbine spacing and U_0 is the mean free stream velocity.

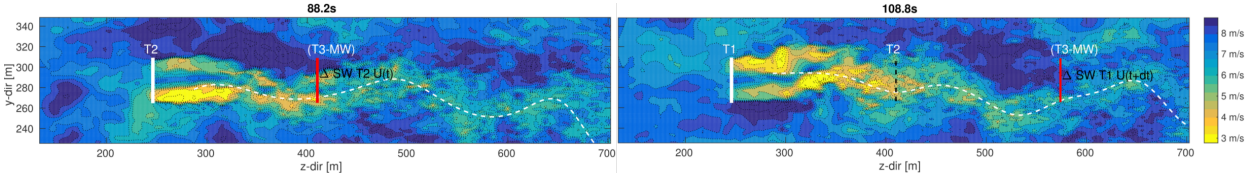

Figure 3. Dominant (instantaneous) wake analysis for the evaluation of the wake accumulation within the DWM framework. The two figures shows the instantaneous velocity contour at hub height at two different time instants. The dash lines represents the wake center obtained from applying the tracking procedure described in [28]. The time difference between the two snapshot is obtained from adopting the Taylor frozen turbulence hypothesis, illustrated by the large high velocity turbulence structure to the left of the two $T3$ locations.

As depicted in Fig. 3, the instantaneous "dominant" wake at the location of the fictitious turbine $T3$ (red section in Fig. 3) is conveniently obtained by analyzing the instantaneous wake of $T2$ at the time instant t and the instantaneous wake of $T1$ at the time instant $t + dt$, where dt is obtained from Taylor hypothesis. This has the advantage of reducing the number of computations in the present study.

3.3.2. First and second modeling approach of linear and quadratic summations
Meanwhile, other model such as FUGA [20] are based on linear summation of single wake deficits obtained at a different inflow conditions than the free stream to account for multiple wake overlapping. This implies first to perform single wake simulations of the most upstream turbine $T1$ at the same inflow conditions as the merged wake ones listed in Table 1.

Additionally, single wake computations of the downstream turbine $T2$ are conducted for a wide range of new inflow conditions to characterize the wake affected inflow. In the present approach, the average reduced wind speed over the rotor area of $T2$ is estimated from power curve reading based on the mean power produced by $T2$ in the merged wake simulation. The increased turbulence intensity generated by the inflow wake of $T1$ is neglected, and therefore the newly generated Mann turbulence field adapted to the reduced wind speed is scaled to reach the same turbulence level as for the merged wake simulation, however, inherently associated to a different turbulent realization. It is assumed that, considering a sufficiently long averaging time, this new realization of turbulence does not affect the average single wake deficits used in the present linear and quadratic summation. The resulting single wake test matrix is shown in Table 2.

3.3.3. The GCL wake superposition model
The analogy between the wake superposition as formulated in the GCL model and the available LES results is more challenging. As opposed to the DWM model, the unsteady inflow velocity of the downwind turbine is affected by the upstream wakes. Furthermore, $T2$ single wake simulations are performed under a different turbulence field, which is incompatible with the GCL formulation.

Table 2. Large Eddy Simulation of the single wake generated by turbine $T1$ and $T2$. Single wake simulations of $T2$ are performed at various mean wind speed characterizing the wake affected inflow generated by $T1$. The change of mean wind speed implies to generate a new set of Mann turbulence field, with the same turbulence level as for the single wake computation of $T1$ but with a new turbulent realization.

	6%	12%	6%	12%	6%	12%	6%	12%
SW $T1$**, 4D-7D** U_0 (m/s)	5	5	8	8	11	11	15	15
SW $T2$**, 4D,** $\tilde{U_0} \neq U_0$ (m/s)	3.95	4.5	6.45	7.24	9.22	10.05	12.84	14.02
SW $T2$**, 7D,** $\tilde{U_0} \neq U_0$ (m/s)	4.32	4.85	7.04	7.62	9.88	10.36	13.04	14.19

From Eq. 7, the merged wake deficit for $n = 2$ rotors ($T1$ and $T2$) at the downstream distance corresponding to a third rotor $T3$ in the GCL superposition framework is given as:

$$\overline{\Delta u}_{T3}(t) = \overline{\Delta u}_{T1}(t)|_{x(T3)}^{U_0(t)} + \overline{\Delta u}_{T2}(t)|_{x(T3)}^{\tilde{U_0}(t)} \tag{10}$$

where the subscript $x(T3)$ corresponds to the downstream distance where the merged wake deficit is estimated, and the superscript U_0 and $\tilde{U_0}$ are the inflow velocity at the first and second rotors, respectively, as defined in Eq. 8. The first term on the right hand side is directly known from the single wake simulations of $T1$ as listed in Table 2. The last term is known from the reduced mean wind speed computations of $T2$, however, under a different turbulence field as previously discussed.

To circumvent this, we apply the equivalence in Eq. 9, so that the single wake computation of $T1$ simulated under the same turbulence field as for the merged wake, is used instead of the $T2$ simulation with the different turbulence realization. However, the difference of inflow conditions between $T1$ and $T2$ simulations requires a scaling of the instantaneous wake deficit.

This scaling procedure can be resumed into in three steps: 1) we first determine the two involved average deficit of $T1$ and $T2$ in their respective meandering frame of reference (MFoR) and at the downstream location of $T3$; 2), we correct each instantaneous velocity deficit of $T1$ by subtracting its average deficit in the MFoR and furthermore adding the average deficit of $T2$ in the MFoR. The final correction is similar to the one performed for the DWM model and is to apply a time shift calculated from Taylor frozen hypothesis on the previously obtained deficit to ensure spatial and temporal correlation of turbulence among the unsteady single wake deficits.

Once the average deficit in the MFoR is known from applying the tracking algorithm as in [28], step 2 gives:

$$\Delta u_{T2}(t)|_{x(T3)}^{\tilde{U_0}(\tilde{t})} \equiv \Delta u_{T1}(t)|_{x(T2)}^{U_0(t)} - \overline{\Delta u}_{T1}^{(M)}|_{x(T2)}^{U_0} + \overline{\Delta u}_{T2}^{(M)}|_{x(T3)}^{\tilde{U_0}} \tag{11}$$

In which the superscript (M) denotes the meandering frame of reference, and $x(T2)$ and $x(T3)$ are the downstream positions of $T2$ and $T3$, respectively.
Applying the time shift of step 3 gives:

$$\Delta u_{T2}(t)|_{x(T3)}^{\tilde{U_0}(t)} \equiv \Delta u_{T1}(t+dt)|_{x(T2)}^{U_0(t)} - \overline{\Delta u}_{T1}^{(M)}|_{x(T2)}^{U_0} + \overline{\Delta u}_{T2}^{(M)}|_{x(T3)}^{\tilde{U_0}} \tag{12}$$

4. Benchmark results and discussion

In this section, the error on the prediction of the average deficit and the available aerodynamic power over the rotor area and at the fictitious location of $T3$ is investigated. It is defined as:

$$\epsilon(CT) = 100 \cdot \left(\frac{Q_{model} - Q_{LES}}{Q_{model}} \right) \tag{13}$$

where Q refers to either integrated deficit or available aerodynamic power from Eq. 2 and 3, respectively. The results are shown as function of the average of the two turbine thrust coefficients for the four tested combinations of turbulence intensity and turbine spacing.

4.1. Linear and quadratic average models

As seen in Fig. 4, the way wakes accumulate is strongly dependent on the thrust force acting on the turbine. Low wind speed associated with a high thrust coefficient typically generates very pronounced wake deficits. Their resulting overlapped wake appears well captured by a quadratic summation with error of the order of 3-5 % for the higher CT configuration. Contrary, at high mean wind speed, the turbine is more 'transparent' to the flow, and linear summation of the very attenuated single wakes seems to be more representative of the merged wake deficit. This is consistent with a linear wake perturbation approach. At moderate wind speed, none of the summation technique is able to capture the merged wake deficit. The quadratic summation underestimates the deficit, whereas the linear summation overestimates it. Thus, averaging both contributions may enhance the agreement over the entire tested wind speed range, similarly to the Horns Rev wake losses study in [4].

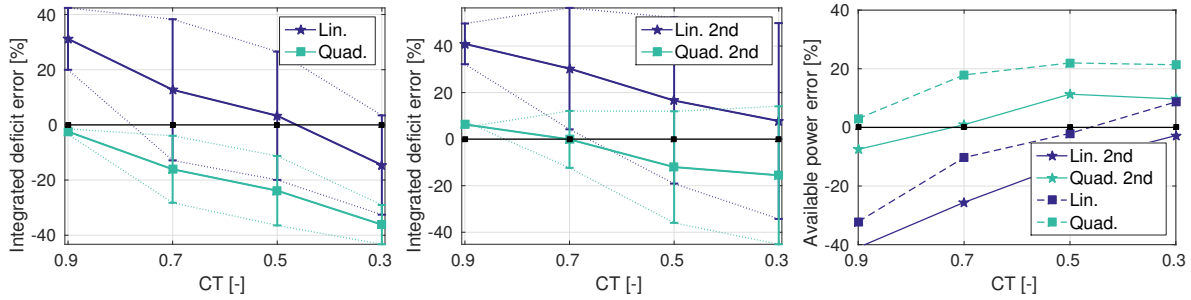

Figure 4. Error on the prediction of the integrated deficit from the steady linear and quadratic models and for the first and second modeling approach (respectively left and center plots). The available aerodynamic power at the downstream location of $T3$ is shown on the right plot. Error bars shows $\pm$ one standard deviation of the error for each thrust (mean wind speed) flow cases.

When considering the more realistic second modeling approach, the downstream single wake contributions is simulated at a reduced average wind speed characterizing the wake affected inflow conditions. Thus, the magnitude of the downstream wake generated by $T2$ is larger, as the CT coefficient of the downstream turbine increases with the reduced incoming wind. Therefore, the quadratic summation prediction error is reduced when using the second modeling approach.

The present results are consistent with earlier observations by Crespo et al. [1], which found that, when considering the superposition of two wakes abreast, that linear superposition of the small velocity deficits in the interference region is robust for predicting the resulting overlapped wake characteristics. Contrary, when considering the situation where two turbines are in a row, the linear superposition assumption overestimates substantially the velocity deficit. Thus, the quadratic summation of Katic et al. [6], proved to perform better for larger deficits. This conclusion is also consistent with the observations made by Gaumond in [3], the semi-empirical superposition law of Smith and Taylor [2] as well as with the wake-wake interaction formulated in the *G.C. Larsen superposition model* [9]

4.2. Dynamic Wake Meandering

Results of the DWM predictions are shown in Fig. 5. It is seen that the overall agreement is fair regardless of the thrust force acting on the turbine. Furthermore, the observed agreement is associated to a systematic overestimation of the available aerodynamic power. It is speculated if the assumption of constant inflow / advection velocity in the DWM framework can result in such power overestimation and therefore will require further investigation, in analogy with the study of the single wake advection velocity in [13].

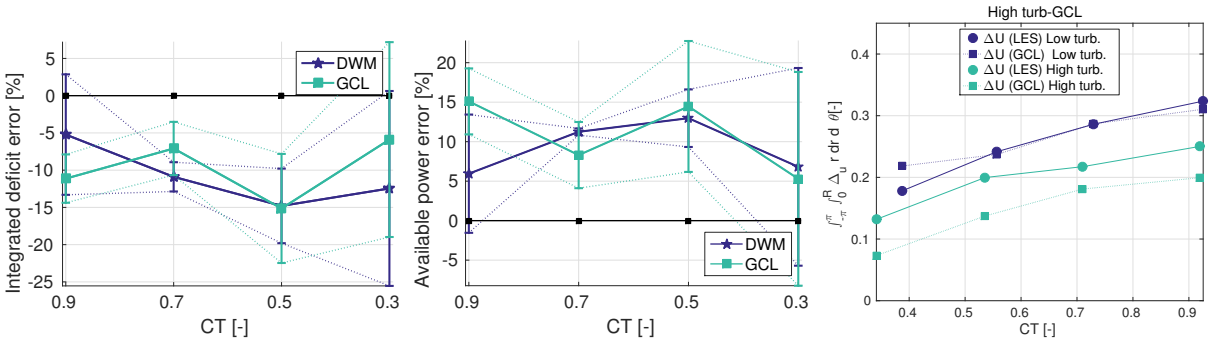

Figure 5. Error on the prediction of the integrated deficit (left) and the available aerodynamic power (middle) at the downstream location of $T3$, based on the Dynamic Wake Meandering and G.C Larsen wake superposition models. Error bars shows ± one standard deviation of the error for each flow case. (Right) Comparison between the G.C Larsen superposition model prediction of the integrated deficit over the rotor with LES results at the location of $T3$ for the low turbulent and high turbulent cases.

4.3. GCL

Finally, the predictions from the GCL model are shown in Fig. 5. This model shows similar overall performance to the DWM one. However, unlike the DWM predictions, the performance of the GCL model varies significantly with respect to the turbulence intensity. An excellent agreement is observed for the low turbulence case whereas the merged wake deficit is significantly underestimated when considering higher turbulence level, as seen in Fig. 5(right). A possible source of uncertainty may come from the implemented wake deficit scaling for the downwind turbine wake. The accuracy of this method can be deteriorated at high turbulence level, where the increased meandering magnitude can affect the performance of the wake tracking procedure and thus, the determination of the two scaling quantities in Eq. 12.

5. Conclusion

In the present work, merging wake engineering models have been evaluated against CFD-LES simulations using the in-house EllipSys3D flow solver for a range of mean wind speeds, turbine spacing and turbulence intensity. The study indicates that wake interaction depends strongly on the relative wake deficit magnitude, i.e. the deficit magnitude normalized with respect to the ambient mean wind speed. Furthermore, the dominant wake assumption within the DWM framework and the parabolic model of G.C. Larsen are both unsteady models capable of predicting the available aerodynamic power in the merged wake flow field with a good degree of accuracy. Simpler and widely used summation techniques such as the linear and quadratic techniques shows an acceptable performance as well, however, typically associated with a higher uncertainties as compared to unsteady models.

The present work will be extended to the study of large rows of turbine more representative of modern wind farm. A new model based on a weighted average combination of linear and quadratic techniques, where the turbine thrust coefficient is used as weighting factor, will be subsequently developed. Furthermore, the added wake turbulence will be quantified and modeled. Sideways wake merging, occurring when the accumulated wake of two turbine rows merged within the wind farm, will also be simulated and compare to the predictions from the wake to wake interaction formulation of the GCL model.

6. Acknowledgments

The major part of this research has been funded and carried out within the DSF FlowCenter project under the Danish Council for Strategic Research contract 2104-09-0026 and the EUDP project "Impact of atmospheric stability conditions on wind farm loading and production"" under contract 64010-0462.

References

[1] A. Crespo, J. Hernández, and S. Frandsen. Survey of modelling methods for wind turbine wakes and wind farms. *Wind Energy*, 1:1–24, 1999.
[2] Smith D. and Taylore G.J. Further analysis of turbine wake development and interaction data. In *Scientific proceedings*, pages 325–331. 13th BWEA Wind Energy Conf. Swansea, 1991.
[3] Mathieu Gaumond. Evaluation and Benchmarking of Wind Turbine Wake Models. 2012.
[4] G. Habenicht. Offshore wake modelling. Presentation at Renewable UK Offshore Wind, 2011.
[5] N. O. Jensen. A note on wind turbine interaction. Technical report, Risø-M-2411, Risø National Laboratory, Roskilde, Denmark, 1983.
[6] I. Katic, J. Høstrup, and N. O. Jensen. A simple model for cluster efficiency. *In proceedings of the European Wind Energy Association Conference and Exhibition (EWEC), Rome*, pages 407–410, 1986.
[7] G. C. Larsen, H. Aa. Madsen, T. J. Larsen, P.-E. Réthoré, and Peter Fuglsang. TOPFARM - A platform for wind farm topology optimization. *Book of Abstracts / Editor: Ivanell S. - Wake conference, Visvy, Sweden*, pages 40–42, 2011.
[8] G. C. Larsen, H. Aa. Madsen, K. Thomsen, and T. J. Larsen. Wake Meandering: A Pragmatic Approach. *Wind Energy*, 11:377–395, 2008.
[9] G.C. Larsen. From solitary wakes to wind farm wind fields a simple engineering approach. Risø-R-1727(EN). Technical report, DTU Wind Energy, Roskilde, Denmark,, 2009.
[10] T.J. Larsen, G.C. Larsen, H.Aa. Madsen, K. Thomsen, and S.M. Pedersen. Comparison of measured and simulated loads for the siemens swt 2.3 operating in wake conditions at the Lillgrund wind farm using HAWC2 and the DWM model. In *Scientific proceedings*, pages –. EWEC Offshore 2015 Copenhagen, 2015.
[11] Torben J. Larsen, Helge Aa. Madsen, Gunner C. Larsen, and Kurt S. Hansen. Validation of the dynamic wake meander model for loads and power production in the egmond aan zee wind farm. *Wind Energy*, 16(4):605–624, 2013.
[12] P.B.S. Lissaman. Energy effectiveness of arbitrary arrays of wind turbines. *Journal of Energy*, 3(6):323–328, 1979.
[13] E Machefaux, G C Larsen, N Troldborg, M Gaunaa, and A Rettenmeier. Empirical modeling of single-wake advection and expansion using full-scale pulsed lidar-based measurements. *Wind Energy*, 2014.
[14] E. Machefaux, G. C. Larsen, N. Troldborg, K.S. Hansen, N. Angelou, T. Mikkelsen, and J. Mann. Investigation of wake interaction using full-scale lidar measurements and large eddy simulation. 2015.
[15] E. Machefaux, N. Troldborg, G. C. Larsen, J. Mann, and H. Aa. Madsen. Experimental and Numerical Analysis of Wake to Wake Interaction in Wind Farms. In *Scientific proceedings*, pages 100–104. EWEC 2012 Copenhagen, 2012.
[16] H. Aa. Madsen, G. C. Larsen, T. J. Larsen, N. Troldborg, and Mikkelsen R. Calibration and Validation of the Dynamic Wake Meandering Model for Implementation in an Aeroelastic Code. *Journal of Solar Energy Engineering*, 2010.
[17] Jakob Mann. Wind field simulation. *Science*, 13(4):269–282, 1998.
[18] J. A. Michelsen. Basis 3d - a Platform for Development of multiblock PDE Solvers. Dept. of Fluid mechanics, DTU. *AFM 92-05*, 1994.
[19] J. A. Michelsen. *Block Structured Multigrid Solution of 2D and 3D elliptic PDE's.* AFM 94-05 - Department of Fluid Mechanics, Technical University of Denmark, 1994.
[20] Søren Ott. *Linearised CFD models for wakes*, volume 1772. 2011.
[21] P.-E. Réthoré and N. N. Sørensen. A discrete force allocation algorithm for modelling wind turbines in computational fluid dynamics. *Wind Energy*, 15:915–926, 2012.
[22] P.-E. Réthoré, P. van der Laan, N. Troldborg, F. Zahle, and N. N. Sørensen. Verification and validation of an actuator disc model. *Wind Energy*, 2013.
[23] N. N. Sørensen. *General Purpose Flow Solver Applied to Flow over Hills.* PhD thesis, Risø National Laboratory., 1995.
[24] L. Ta Phuoc, R. Lardat, M. Coutanceau, and G. Pineau. Recherche et analyse de modèles de turbulence de sous mailles adaptés aux écoulements instationnaires décollés. LIMSI, France. Technical report, LIMSI Report 93074, 2002.
[25] A.M. Hansen T.J.Larsen. *HAWC2 - User manual.* DTU-Risø-R-1597, 2007.
[26] N. Troldborg, G. C. Larsen, H. Aa. Madsen, K. S. Hansen, J. N. Sørensen, and R. Mikkelsen. Numerical Simulations of Wake Interaction between Two Wind Turbines at Various Inflow Conditions. *Wind Energy, 14, doi: 10.1002/we.433*, pages 859–876, 2010.
[27] N. Troldborg, J.N. Sørensen, R. Mikkelsen, and N.N Sørensen. A simple atmospheric boundary layer model applied to large eddy simulations of wind turbine wakes. *Wind Energy*, 2013.
[28] J. J. Trujillo, F. Bingöl, G. C. Larsen, J. Mann, and M. Kuehn. Lidar Measurements of Wake Dynamics, part 2: Two-dimensional scanning. *Wind Energy*, 14:61–75, 2011.